J. Chem. Eng. Data **2009,** *54,* 3079–3081

Adsorption of Nitrous Oxide on Activated Carbons

Yong Peng, Fumin Zhang, Chunhui Xu, Qiang Xiao, Yijun Zhong, and Weidong Zhu*

Key Laboratory of the Ministry of Education for Advanced Catalysis Materials, Institute of Physical Chemistry, Zhejiang Normal University, Jinhua 321004, P. R. of China

The adsorption equilibria of nitrous oxide (N_2O) on three commercial activated carbons were systematically investigated by means of a volumetric method at pressures up to 101 kPa and temperatures ranging from (195 to 323) K. The multiple-process adsorption equilibrium model appropriately describes the equilibrium data over the whole range of the applied conditions. The estimated total adsorption capacity of N_2O is higher for activated carbon which possesses a higher pore volume determined by N_2 adsorption at 77 K. The thermodynamic properties such as the adsorption equilibrium constant and enthalpy associated with adsorption were derived to characterize interactions between adsorbate and adsorbent.

Introduction

Nitrous oxide (N_2O) is a strong greenhouse gas and has aroused great attention.[1,2] The potential for global warming and destruction of ozone has spurred the development of various strategies to decrease the concentration of N_2O in the atmosphere. One of the methodologies is of direct decomposition over effect catalysts, either by an end-of-pipe treatment or by the reuse of N_2O in the tail gas for other reactions to other valuable products.[2−4] An adsorption-based process is an alternative to the recovery of N_2O in nitric acid plants where diluted N_2O streams (0.05 % to 0.2 % by volume) are present to produce a concentrated stream (> 5 % by volume) or to store N_2O which is characterized by high concentrations (> 30 % by volume) in exhausts from adipic acid.[5] Activated carbon or post-treated activated carbon is a promising adsorbent due to its unique advantages such as large specific surface area and inherently large pore volume, resulting in a large adsorption capacity.[6] Therefore, activated carbon is the most widely used adsorbent in adsorption-based processes.[6,7]

For industry applications of gas adsorption and recovery as well as in the characterization of porous activated carbon, it is essential to acquire information on adsorption equilibria, which is a prerequisite to understand an adsorption process. Experimentally, however, only limited work has been carried out on a comparative and systematic investigation on the adsorption of N_2O on different types of activated carbon, although several hundred sets of data for numerous adsorbates on carbon materials have been measured, and these data are accumulated in a handbook by Valenzuela and Myers.[8]

This paper presents experimental results for the adsorption isotherms of N_2O on three commercial activated carbons determined by a volumetric method. In addition, thermodynamic properties such as the adsorption equilibrium constant and enthalpy associated with adsorption are determined to characterize interactions between adsorbate and adsorbent.

Experimental Section

Adsorption Measurements. A Micromeritics ASAP 2020 gas adsorption analyzer (stainless steel version) was used to accurately measure the adsorption isotherms of N_2O on three adsorbents in the pressure range from (0.01 to 101) kPa. The instrument was equipped with a molecular drag vacuum pump and two different pressure transducers to enhance the sensitivity in the low-pressure range, which is especially useful in adsorption studies on adsorbents containing micropores. The static-volumetric technique was used to determine the volume of gas adsorbed at different partial pressures: upon adsorption, a pressure decrease was observed in the gas phase, which was a direct measure of the amount adsorbed.

Table 1. Textural Properties of the Activated Carbons Investigated

adsorbent	$S_{BET}/m^2 \cdot g^{-1}$	$V_{total}/cm^3 \cdot g^{-1}$	$V_{micro}/cm^3 \cdot g^{-1}$
Kureha	1300	0.560	0.560
Ovcls	1055	0.501	0.397
Vruf	1330	0.810	0.040

The sample cell was loaded with approximately 200 mg of the adsorbent particles. Prior to the adsorption measurements, the adsorbent particles were outgassed in situ in a vacuum at 623 K for 16 h to remove any adsorbed impurities. The obtained dry sample mass was used in the calculation of isotherm data. Adsorption measurements were subsequently carried out at four different temperatures (195 K, 273 K, 293 K, and 323 K). The temperatures were controlled within ± 0.3 K using solid carbon dioxide and an ice−water mixture as coolants to fix the temperatures at (195 and 273) K, respectively, and a circulating water bath was used to control the temperatures at (293 and 323) K within ± 0.1 K.

Adsorbents and Adsorbates. Three commercial activated carbons were used as the adsorbents in this study. They were purchased from the Kureha Chemical Industry and Calgon Carbon Corporation (brand codes: OVC-LS and VRU-F). These activated carbons are referred to as Kureha carbon, Ovcls carbon, and Vruf carbon, respectively. The textural properties of Kureha carbon were reported elsewhere.[9] Kureha carbon is a purely microporous material. The textural properties of Ovcls carbon and Vruf carbon were determined by the adsorption isotherms of N_2 at 77 K measured with a Micromeritics ASAP 2020 gas adsorption analyzer. The textural properties of all the investigated activated carbons are summarized in Table 1. Ovcls carbon contains primarily micropores and a small quantity of mesopores, while Vruf carbon

---

* Corresponding author. Tel./Fax: +86-579-82282932. E-mail: weidongzhu@zjnu.cn.

10.1021/je9001625 CCC: $40.75

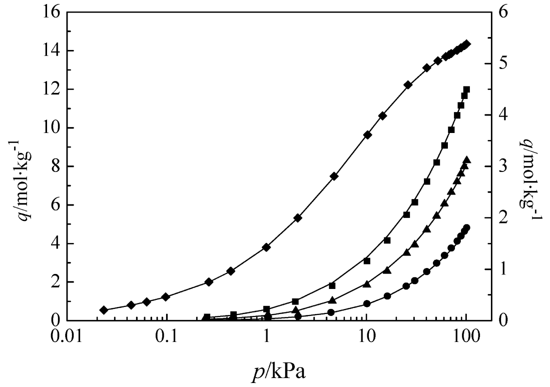

Figure 1. Adsorption isotherms of N_2O on Kureha carbon. Lines are the three-process adsorption equilibrium model correlation. ◆, 195 K; ■, 273 K; ▲, 293 K; ●, 323 K. The isotherm at 195 K corresponds to the left *y*-axis, and the isotherms at other temperatures correspond to the right *y*-axis.

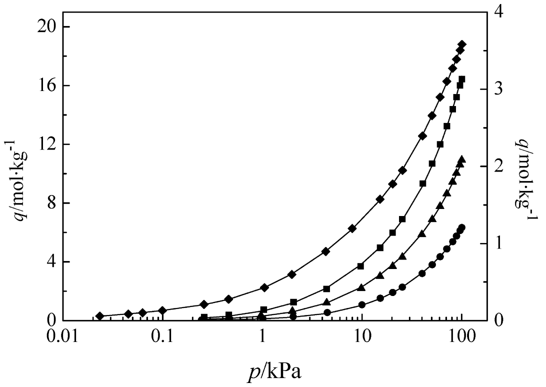

Figure 3. Adsorption isotherms of N_2O on Vruf carbon. Lines are the three-process adsorption equilibrium model correlation. ◆, 195 K; ■, 273 K; ▲, 293 K; ●, 323 K. The isotherm at 195 K corresponds to the left *y*-axis, and the isotherms at other temperatures correspond to the right *y*-axis.

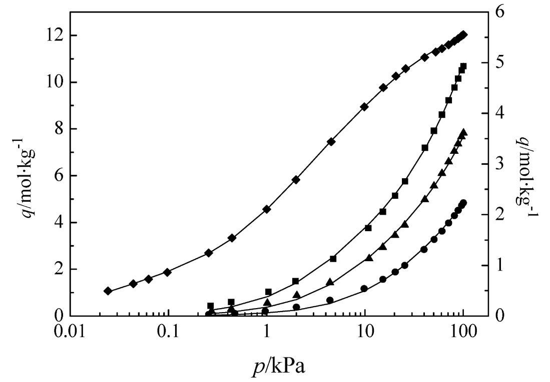

Figure 2. Adsorption isotherms of N_2O on Ovcls carbon. Lines are the three-process adsorption equilibrium model correlation. ◆, 195 K; ■, 273 K; ▲, 293 K; ●, 323 K. The isotherm at 195 K corresponds to the left *y*-axis, and the isotherms at other temperatures correspond to the right *y*-axis.

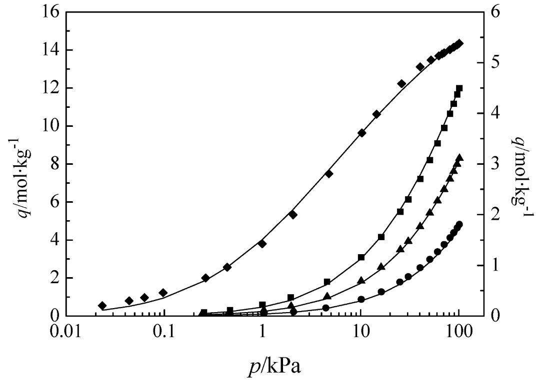

Figure 4. Adsorption isotherms of N_2O on Kureha carbon correlated by the Tóth model. ◆, 195 K; ■, 273 K; ▲, 293 K; ●, 323 K. The isotherm at 195 K corresponds to the left *y*-axis, and the isotherms at other temperatures correspond to the right *y*-axis.

possesses both micro- and mesopores and only a small amount of micropores contribute to its total pore volume.

The gaseous adsorbate nitrous oxide with a purity over 99.99 % was used without further purification. Ultrahigh purity (> 99.999 %) helium was used to determine the free space of the sample cell.

Isotherm Model. For practical utility, the experimental data should be described by an analytical expression that includes temperature dependency. Various empirical or semiempirical models have been proposed to fit isotherm data in adsorption science. The multiple-process adsorption equilibrium model, which was introduced by Drago et al.[10−13] to analyze gas adsorption equilibria in porous carbonaceous materials and zeolites, is based on the fact that an adsorbent consists of several different size pores, and it is reasonable to premise that adsorption involves a series of elementary equilibrium processes that differ in their enthalpy and entropy. Each process may be a heterogeneous grouping of pores whose affinities are too close to be discriminated by the accuracy of experimental measurements. As each equilibrium process is described by an equilibrium constant, K_i, and a finite capacity, q_i, the total adsorption isotherm is given by eq 1

$$q = \sum_{i=1}^{n} \frac{q_i^{\mathrm{sat}} K_i p}{1 + K_i p} \qquad (1)$$

where q is the total amount adsorbed; q_i^{sat} is an intrinsic property of the adsorbent reflecting the capacity for process i; K_i is the associated equilibrium constant; and p is the equilibrium pressure. The quantity q_i^{sat} is temperature independent as it represents a saturation capacity for one adsorption process. The equilibrium constant K_i is temperature dependent and effectively describes the extent to which a particular type of pore fills at a given temperature. The parameter K_i taking the van't Hoff relation for the adsorption affinity can be written as

$$K_i = K_{i0} \exp\left[\frac{-\Delta H_{\mathrm{ads},i}}{R_{\mathrm{g}} T_0}\left(\frac{T_0}{T} - 1\right)\right] \qquad (2)$$

where K_{i0} is the adsorption affinity at reference temperature T_0; $\Delta H_{\mathrm{ads},i}$ is a measure of the enthalpy of adsorption; R_{g} is the universal gas constant; and T is the temperature studied. The lowest temperature investigated, 195 K, is used as T_0, since the measured isotherm at this temperature covers the widest range of loading.

Results and Discussion

The adsorption isotherm data of N_2O on the three commercial activated carbons are given by the points in Figures 1 to 3. All the isotherms exhibit a type-I adsorption isotherm (Brunauer classification) over the temperature and pressure range investigated.

The measured isotherm data were correlated by the multiple-process adsorption equilibrium model. The nonlinear parameter estimation was carried out in two steps using a combined fitting method.[14] Three processes were required to obtain good fits to the experimental data. First, the six parameters in eq 1, referred to as q_1^{sat}, q_2^{sat}, q_3^{sat}, K_{10}, K_{20}, and K_{30}, were extracted from the isotherm data at T_0, i.e., 195 K. Second, the parameter $\Delta H_{\mathrm{ads},i}$ for each adsorption process was estimated from the isotherm data at all the

Table 2. Estimated Values of Adsorption Isotherm Parameters in the Three-Process Adsorption Equilibrium Model and Their Standard Deviations (95 % Confidence Limit)

parameter	process	Kureha carbon	Ovcls carbon	Vruf carbon
$q^{\mathrm{sat}}/\mathrm{mol \cdot kg^{-1}}$	1	1.109 ± 0.223	1.887 ± 0.188	0.783 ± 0.084
	2	4.027 ± 0.502	6.107 ± 0.647	5.525 ± 0.180
	3	10.183 ± 0.610	4.665 ± 0.692	30.622 ± 0.751
	Total	15.319 ± 1.335	12.659 ± 1.527	36.930 ± 1.014
$K_0/\mathrm{kPa^{-1}}$	1	27.760 ± 10.065	39.813 ± 9.828	19.979 ± 5.027
	2	0.902 ± 0.266	0.665 ± 0.142	0.284 ± 0.026
	3	0.092 ± 0.007	0.062 ± 0.015	0.007 ± 0.000
$-\Delta H_{\mathrm{ads}}/\mathrm{kJ \cdot mol^{-1}}$	1	28.978 ± 0.237	29.708 ± 0.126	28.246 ± 0.145
	2	25.389 ± 0.280	26.777 ± 0.542	25.671 ± 0.368
	3	23.095 ± 0.303	18.427 ± 1.146	16.496 ± 0.356

temperatures by eqs 1 and 2. The isotherm data can be appropriately described by the three-process adsorption equilibrium model, as shown in Figures 1 to 3 by the drawn lines.

Other isotherm models, such as the Tóth, Unilan, and Dubinin−Radushkevich (DR) models,[15] which are frequently used to describe adsorption equilibria of various adsorbates on different types of activated carbon, have also been considered. The Unilan and DR models deviate from the measured isotherm data to a great extent in the current case. In comparison with the Unilan and DR models, the Tóth model gives a relatively better description for N_2O adsorption on the three activated carbons investigated. Figure 4 shows an example for the isotherms of N_2O on Kureha carbon correlated by the Tóth model. However, as seen from Figure 4, the line predicted by the Tóth model is slightly below the experimental data points at 195 K in the lower pressure range, while at moderate pressures the correlated isotherm is somehow higher. This could be due to the high degrees of heterogeneity for the activated carbon materials investigated, and the Tóth model with three fitting parameters cannot properly describe this heterogeneity, resulting in the deviation of model predictions from isotherm data. In summary, the three-process adsorption equilibrium model describes the present case the best over the full range.

The values of q_i^{sat}, K_{i0}, and $-\Delta H_{\mathrm{ads},i}$ extracted by the three-process adsorption equilibrium model are summarized in Table 2. The process capacity, q_i^{sat}, reflects the number of moles of adsorbate that can be adsorbed by pores with a specific width or range of widths. Summing the adsorption capacities for all the three processes results in the total saturation amount adsorbed, $q_{\mathrm{total}}^{\mathrm{sat}}$, which is also presented in Table 2. The $q_{\mathrm{total}}^{\mathrm{sat}}$ value is in the order of adsorbent as follows: Vruf carbon > Kureha carbon > Ovcls carbon, which is in line with the increasing total pore volume of these adsorbents (see Table 1).

The enthalpy of adsorption, $\Delta H_{\mathrm{ads},i}$, describes the extent of adsorption affinity. The extracted $-\Delta H_{\mathrm{ads},i}$ value decreases along with the adsorption process. On the same adsorbent, adsorption first occurs in micropores due to the superimposed interaction potentials from opposite surfaces within the carbon pores that generate the significantly larger value of $-\Delta H_{\mathrm{ads},1}$. Along with adsorption, the adsorption affinity decreases gradually and generates the smaller $-\Delta H_{\mathrm{ads},2}$ value and the even smaller $-\Delta H_{\mathrm{ads},3}$ value. The value of $-\Delta H_{\mathrm{ads},i}$ for processes 1, 2, and 3, presented in Table 2, gradually decreases for N_2O on all three activated carbons investigated. This further supports the consideration of the change of adsorption potential along with the adsorption process.

To recover N_2O in nitric acid plants where diluted N_2O streams (0.05 % to 0.2 % by volume) are present,[5] Kureha carbon and Ovcls carbon could be suitable adsorbents because they possess mainly micropores, in which the interactions between N_2O and pore walls are stronger, resulting in higher amounts adsorbed at low partial pressures of the adsorbate. On the other hand, to store N_2O that is characterized by high concentrations (> 30 % by volume) in exhausts from adipic acid,[5] Vruf carbon, which possesses mainly mesopores, could be an alternative adsorbent because it exhibits the greatest adsorption capacity for N_2O.

Conclusions

The adsorption isotherms of N_2O on Kureha carbon, Ovcls carbon, and Vruf carbon have been accurately measured up to 101 kPa and at temperatures in the range of (195 to 323) K. A three-process adsorption equilibrium model gives the best description of the measured adsorption isotherm data on all three adsorbents investigated. The present results might be useful for modeling adsorption-based processes to concentrate tail-gas streams containing diluted N_2O or to recover N_2O with high concentrations in exhausts from chemical plants.

Literature Cited

(1) Rodhe, H. A comparison of the contribution of various gases to the greenhouse effect. *Science* **1990**, *248*, 1217–1219.

(2) Pérez-Ramírez, J. Catalyzed N_2O activation: promising (new) catalysts for abatement and utilization; Ph.D. Thesis, Delft University of Technology: The Netherlands, 2002.

(3) Pérez-Ramírez, J.; Kapteijn, F.; Mul, G.; Moulijn, J. A. Superior performance of ex-framework FeZSM-5 in direct N_2O decomposition in tail-gases from nitric acid plants. *Chem. Commun.* **2001**, 693–694.

(4) Panov, G. I. Advances in oxidation catalysis: oxidation of benzene to phenol by nitrous oxide. *CATTECH* **2000**, *4*, 18–32.

(5) Groen, J. C.; Pérez-Ramírez, J.; Zhu, W. Adsorption of nitrous oxide on silicalite-1. *J. Chem. Eng. Data* **2002**, *47*, 587–589.

(6) Yang, R. T. *Adsorbents: fundamentals and applications*; John Wiley & Sons: NJ, 2003.

(7) Bansal, R. C.; Goyal, M. *Activated carbon adsorption*; Taylor & Francis: Boca Raton, 2005.

(8) Valenzuela, D. P.; Myers, A. L. *Adsorption equilibrium data handbook*; Prentice-Hall: NJ, 1989.

(9) Zhu, W.; Groen, J. C.; Kapteijn, F.; Moulijn, J. A. Adsorption of butane isomers and SF_6 on Kureha activated carbon. 1. Equilibrium. *Langmuir* **2004**, *20*, 5277–5284.

(10) Drago, R. S.; Burns, D. S.; Lafrenz, T. J. A new adsorption model for analyzing gas-solid equilibria in porous materials. *J. Phys. Chem.* **1996**, *100*, 1718–1724.

(11) Drago, R. S.; Kassel, W. S.; Burns, D. S.; McGilvray, J. M.; Showalter, S. K.; Lafrenz, T. J. Multiple equilibria analyses of gas-porous solid isotherms. *J. Phys. Chem. B* **1997**, *101*, 7548–7555.

(12) Drago, R. S.; Webster, C. E.; McGilvray, J. M. A multiple-process equilibrium analysis of silica gel and HZSM-5. *J. Am. Chem. Soc.* **1998**, *120*, 538–547.

(13) Webster, C. E.; Cottone, A.; Drago, R. S. Multiple equilibrium analysis description of adsorption on Na-Mordenite and H-Mordenite. *J. Am. Chem. Soc.* **1999**, *121*, 12127–12139.

(14) Zhu, W.; Groen, J. C.; van Miltenburg, A.; Kapteijn, F.; Moulijn, J. A. Comparison of adsorption behaviour of light alkanes and alkenes on Kureha activated carbon. *Carbon* **2005**, *43*, 1416–1423.

(15) Do, D. D. *Adsorption analysis: equilibria and kinetics*; Imperial College Press: London, 1998.

Received for review February 8, 2009. Accepted May 16, 2009.

JE9001625